

Received March 22, 2021, accepted April 1, 2021, date of publication April 8, 2021, date of current version April 19, 2021.

Digital Object Identifier 10.1109/ACCESS.2021.3071820

A Virtually Coupled Metro Train Platoon Control Approach Based on Model Predictive Control

ZIYU WU^{1,2,3}, CHUNHAI GAO^{2,3}, AND TAO TANG¹, (Senior Member, IEEE)

¹School of Electronic and Information Engineering, Beijing Jiaotong University, Beijing 100044, China

²Traffic Control Technology Company Ltd., Beijing 100070, China

³National Engineering Laboratory for Urban Rail Transit Communication and Operation Control, Beijing 100044, China

Corresponding author: Ziyu Wu (wuzyca@126.com)

This work was supported by the Beijing Postdoctoral Research Foundation under Grant 2020-22-091.

ABSTRACT In this paper, a virtually coupled train formation (VCTF) control method based on the model predictive control (MPC) framework is proposed. The train track spacing error, velocity error, and riding comfort are chosen as the optimization goals, and the constraints of line speed, collision avoidance of the train platoon, traction/braking performance, and string stability are considered. The virtual coupling operation control problem is converted into a quadratic programming problem with constraints. This paper also proposes a coasting control strategy to improve the output of the MPC controller. Simulation results show that compared with the proportional derivative controller, the proposed control method can simultaneously reduce the tracking error and output acceleration, reducing running energy consumption. A study of a metro line is chosen to analyze the VCTF operation performance, and the simulation results show that the VCTF operation mode can improve the peak capacity and quality of service of flat hours compared with the communication-based train control operation mode.

INDEX TERMS Virtually coupled, metro train platoon, model predictive control.

I. INTRODUCTION

The increasing scale of urban environments is increasing the separation between a person's occupation and residence. Therefore, the travel demands of commuters are growing, and traffic congestion is increasingly prominent. As one of the leading transportation modes of urban public transport, the metro plays an essential role in relieving traffic pressure and overcoming urban congestion. To cope with changes in passenger flows, subway operators adjust train departure intervals, but the effects of such adjustments are limited. For example, the Beijing Metro Line 1 peak departure interval is 90 s during rush hour. However, the metro capacity remains insufficient. The departure interval increases to 4 min during the low-traffic period to improve the train utilization ratio, which increases the waiting time of passengers and reduces the quality of service.

Under the condition of the limited track and train resources, a fixed train formation cannot meet the operational requirements of a tidal passenger flow. The organization shift2Rail has proposed splitting an existing train formation into several

The associate editor coordinating the review of this manuscript and approving it for publication was Mohamad Afendee Mohamed¹.

minimum modules containing a power unit to improve the flexibility of metro operation. The train modules are connected via communication and separated according to the relative braking distance. Several connected modules form one virtually coupled train formation (VCTF) for coordinated operation. The number of train modules in one VCTF can be adjusted to match the metro transport capacity with passengers' travel demands more accurately and flexibly. At rush hour, the number of train modules in one VCTF increases, increasing the subway capacity. During a low-traffic period, the number of train modules decreases to increase the train utilization with the same departure interval, and the passenger waiting time is improved [1], [2]. A schematic of the VCTF is shown in Fig. 1. Train modules 1, 2, ..., k exchange operational information via vehicle-to-vehicle (V2V) communication, and the modules are separated according to the relative braking distance to form a virtually coupled fleet. The ground control center uniformly distributes the track resources via a vehicle-to-infrastructure (V2I) communication approach for all train modules as a convoy.

It is necessary to solve the distributed cooperative driving and control problem of the train modules. The cooperative operation of different cars in a platoon has been studied and

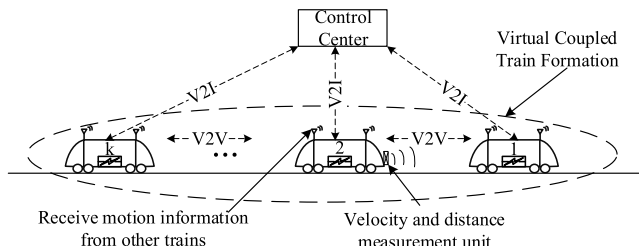


FIGURE 1. Virtually coupled train formation diagram.

applied to road traffic. According to the research, a vehicle platoon can improve the road capacity and reduce traffic congestion by keeping cars traveling at the same speed and distance [3], [4]. Owing to the speed fluctuation of the leader car, the cooperative control of the following vehicles remains challenging. In addition, the VCTF cooperative control task is not a single-target control problem. First, the trains in the formation must track the speed of the leading train. Second, when adjusting the accelerations of the trains, it is necessary to consider the passenger riding comfort and avoid extensive changes in the acceleration rate. Finally, when a train is operating between stations, the running energy cost should be minimal and avoid unnecessary energy consumption due to frequent acceleration and braking operations. These multiple control objectives are relevant and must be balanced. The trains in the formation must meet the safety constraints and avoid collision of adjacent trains. In case of emergency, it must be ensured that each train can stop safely. Thus, it is necessary to supervise the train spacing in real time to ensure that it is larger than the relative braking distance. Therefore, the cooperative control task of a virtually coupled formation train is a multiobjective optimization control problem with constraints. It is necessary to find an optimal driving strategy to minimize the tracking spacing error, jerk, and energy consumption under safe spacing constraints.

Several studies have been conducted to realize the operational mode of VCTF. In [5], the concept of virtually coupled train operation was first proposed to enhance the capacity and flexibility of European freight railways. The basic concept and system structure of virtual connections were analyzed in [6]. In recent years, shift2Rail has proposed virtual connectivity as one of the most critical innovations in the next generation of signal systems. The application and market potential of virtual connections have been analyzed in [7]. For tracking safety of close-range train unit formation, [8] proposed a topological manifold-based monitoring method and derived safety monitoring theorems to ensure virtual coupling control logic safety. In [9], the blockchain method was adopted to monitor and predict the position of a virtually coupled train on the line to avoid train route conflicts, and a corresponding conflict handling strategy was formulated. A control law including a communication delay time was designed, and Yalmip tools were used to solve the controller parameters corresponding to the optimal convergence speed [10]. In [11], virtual coupling capacity was compared with the traditional communication-based train control (CBTC) signal system,

and the results demonstrated this capacity via virtual coupling gains under various operational scenarios. In [12], a model predictive control (MPC) method was used to design a train formation following controller, and a simulation study of Ho Chi Minh City Line 1 was conducted. A distributed optimal control method of multiple high-speed trains was proposed in [13] to overcome communication constraints and realize efficient speed control. The requirement of communication among virtually coupled train sets was analyzed in [14].

Many studies have been conducted in the field of car platoon control. In [15], a two-layer control architecture for a heavy-duty vehicle platoon was proposed, and the simulation results showed possible fuel savings of 12% for follower vehicles. In [16], a hierarchical decision and control framework for a truck platoon was proposed to solve the multiple merging problem during mandatory lane changes. An optimized information flow topology model and an adaptive proportional derivative (PD) controller were proposed in [3] to enhance the stability of platoon control under the unreliable V2V communications condition. In [17], a distributed MPC with multiple objectives of a heterogeneous vehicle platoon was presented, and the fuel consumption table was calculated offline to reduce the computational burden. To ensure the internal stability and string stability of a platoon, [4], [18]–[20] derived and proved a sufficient condition for local stable and string stability that guides the selection of controller parameters of feedback gains and the desired time gap. Because the vehicle system parameter is vital to the control of a platoon, [21] developed a realistic and collision-free car-following model for vehicles with adaptive cruise control–cooperative adaptive cruise control. In [22], a dual unscented Kalman filter approach was proposed to obtain inertial vehicle parameters.

Related research on existing references has focused on communication topology, system architecture, operation scenarios, and capacity analysis. In terms of studying the control strategy of a virtually coupled train, most studies consider only the following distance error of the formation-following vehicle as a control target, yet they ignore the comfort level and energy consumption of the train. Most current studies do not consider the line velocity limit or the train traction and braking system constraints when designing a virtual coupling controller. Moreover, because the metro operational requirements are flexible and efficient, no theoretical or simulation studies have been conducted that provide a control method suitable for the metro operation. Therefore, considering the need for the virtually coupled formation operation of subway trains, this paper proposes a design method for cooperative control of a virtually coupled metro train formation.

The remainder of this paper is organized as follows. Section II presents the dynamic model of a virtually coupled train platoon. Section III introduces the MPC approach and coasting strategy of a virtually coupled train platoon for multiple objectives control with constraints. In Section IV, the simulation results are discussed, followed by the conclusions and an outlook on future work in Section V.

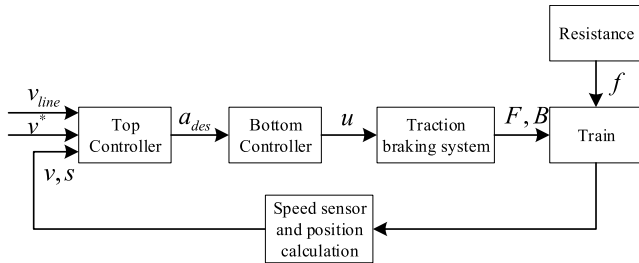


FIGURE 2. Metro train automatic control schema.

II. VIRTUALLY COUPLED TRAIN MOTION MODEL

A. TRAIN MOTION MODEL

A block diagram of the subway automatic train operation (ATO) system is shown in Figure 2.

According to the error between the current train speed v and the recommended speed v^* , a controller (e.g., PD controller, fuzzy controller, and sliding mode controller) is used to calculate the expected acceleration of the train. By examining the train traction and braking characteristic curve table, the expected acceleration is sent to the control command u and then transferred to the traction/braking actuator for execution. The corresponding traction T or braking force B acting on the train is then adjusted. Under the forces of T , B , and the basic running resistance f , the train completes the specified movement.

According to Newton's law of kinematics, the train motion model can be expressed as

$$\begin{cases} \dot{s}_i(t) = v_i(t) \\ m_i \dot{v}_i(t) = T_i(u, v) - f_i(s, v) - B_i(u, v) \end{cases} \quad (1)$$

where S_i , v_i , m_i , T_i , B_i , and f_i denote the position, speed, train quality, traction force, braking force, and running resistance of train i , respectively. The basic running resistance of the train includes wind, mechanical friction, ramp, and bend resistance. According to the Davis equation, the running resistance of the train can be expressed as

$$f_i(s, v) = a + b \times v_i + c \times v_i^2 + m_i g \sin \theta(s) + \frac{A}{r(s)} \quad (2)$$

where a , b , and c represent the wind resistance coefficients determined by the train type. A is the bend resistance coefficient that is obtained experimentally, θ_s is the slope of the line, and $r(s)$ is the radius of the bend.

The train traction/braking system response model is considered as a second-order system that can be expressed as

$$\ddot{s}_i = \frac{1}{\tau s + 1} a_{ides} \quad (3)$$

where τ is the lag time constant of the train, and a_{ides} is the desired acceleration calculated by the automatic driving controller.

B. MULTITRAIN VIRTUALLY COUPLED MOTION MODEL

A schematic of a virtually coupled train formation is shown in Figure 3. Trains 1, 2, ..., m form a platoon, and train 1 is the leader train that operates under the control of the ATO

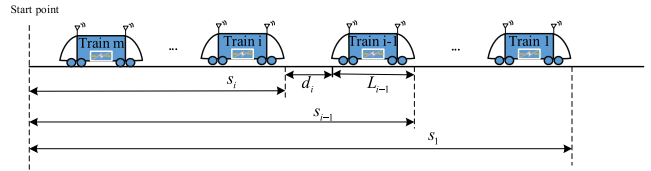


FIGURE 3. Virtually coupled train platoon diagram.

according to the train schedule. Trains 2, 3, ..., m follows the previous train with the desired clearance.

According to [13], the desired distance between the trains in the platoon is obtained using the constant time gap spacing model to ensure the efficiency and stability of the train platoon. The ideal distance between trains i and $i - 1$ can be expressed as

$$d_{ides} = k_t \times v_i + d_0 \quad (4)$$

where k_t is the tracking time coefficient, and d_0 is the safe distance margin.

Assuming that the sampling time is T_s , Eq. (3) is discretized according to the Euler method. The train model in the discrete-time domain can be expressed as follows:

$$a_i(k+1) = \left(1 - \frac{T_s}{\tau}\right) a_i(k) + \frac{T_s}{\tau} u_i(k) \quad (5)$$

where $u_i(k)$ is the control input at step k , and $a_i(k)$ is the acceleration of train i at step k .

The distance between trains i and $i - 1$ and the velocity difference, acceleration, and speed are selected as the state quantity, and the acceleration of train $i - 1$ is taken as the measurable disturbance term. According to Eqs. (1) and (5), the state-space equation of train i is constructed as follows:

$$\begin{aligned} x_i(k+1) &= Ax_i(k) + B_u u_i(k) + B_w w_i(k) + Z \\ y_i(k) &= Cx_i(k) \end{aligned} \quad (6)$$

where $x_i = [\Delta a_i \Delta v_i a_i j_i]^T$ and $w_i = a_{i-1}$; A , B_u , B_w , and Z represent the system coefficient matrix and can be described as

$$\begin{aligned} A &= \begin{bmatrix} 1 & T_s & -k_t T_s & 0 & 0 \\ 0 & 1 & -T_s & 0 & 0 \\ 0 & 0 & T_s & 1 & 0 \\ 0 & 0 & 1 - T_s/\tau & 0 & 0 \\ 0 & 0 & 0 & -\frac{1}{\tau} & 0 \end{bmatrix}, \quad B_u = \begin{bmatrix} 0 \\ 0 \\ 0 \\ T_s/\tau \\ \frac{1}{\tau} \end{bmatrix} \\ B_w &= \begin{bmatrix} 0 \\ T_s \\ 0 \\ 0 \\ 0 \end{bmatrix}, \quad Z = \begin{bmatrix} -d_0 \\ 0 \\ 0 \\ 0 \\ 0 \end{bmatrix} \end{aligned} \quad (7)$$

An integral is introduced into the state-space equation to eliminate the static error. Eq. (6) may be rewritten in an incremental form, and the incremental state equation of train i can be expressed as

$$\begin{aligned} \Delta x_i(k+1) &= A \Delta x_i(k) + B_u \Delta u_i(k) + B_w \Delta w_i(k) \\ y_{ic}(k) &= C_c \Delta x_i(k) + y_{ic}(k-1) \end{aligned} \quad (8)$$

where y_{ic} is the controlled output variables, and C_c is the controlled output coefficient matrix. Because the control objectives of a virtually coupled train platoon are formation efficiency and passenger comfort, the controlled output variables can be described as $y_{i,c}(k) = [\Delta d_i(k) \ \Delta v_i(k) \ j_i(k)]^T$, and $j_i(k)$ is the rate of change in the train acceleration. Thus, C_c is

$$C_c = \begin{bmatrix} 1 & 0 & 0 & 0 & 0 \\ 0 & 1 & 0 & 0 & 0 \\ 0 & 0 & 0 & 0 & 1 \end{bmatrix} \quad (9)$$

III. PROBLEM STATEMENT

A. PREDICTION EQUATION

The prediction control method predicts a future dynamic output based on the current measurement state and motion model. The prediction time domain is set as p , the control time domain is m , and to reduce the prediction equation calculation, the following assumptions are made: 1) $m \leq p$, and the control quantity is zero outside the control time domain, and 2) detectable disturbances remain unchanged during the prediction of the time domain.

According to the current measured state $x(k)$ and the last step measured state $x(k-1)$, the initial state increment $\Delta x(k)$ can be calculated. The estimated value of the states in the prediction time domain can be expressed as

$$\left\{ \begin{array}{l} \Delta x_i(k+1|k) = A\Delta x_i(k) + B_u\Delta u_i(k) + B_w\Delta w_i(k) \\ \Delta x_i(k+2|k) = A^2\Delta x_i(k) + AB_u\Delta u_i(k) \\ +B_u\Delta u_i(k+1) + AB_w\Delta w_i(k) \\ \vdots \\ \Delta x_i(k+p|k) = A^p\Delta x_i(k) + A^{p-1}B_u\Delta u_i(k) \\ +A^{p-2}B_u\Delta u_i(k+1) + \dots \\ +A^{p-m}B_u\Delta u_i(k+m-1) + A^{p-1}B_w\Delta w_i(k) \end{array} \right. \quad (10)$$

By rewriting Eq. (10) in matrix form, the state quantity in the prediction time domain can be expressed as follows:

$$X_p = A_p\Delta x_i(k) + B_{up}\Delta U_i(k) + B_{wp}\Delta w_i(k) \quad (11)$$

where X_p represents the p -step prediction state vector, $\Delta U_i(k)$ represents the input vector, and A_p , B_{up} , and B_{wp} represent the recursive coefficient matrix.

Similarly, the output of the future p -step prediction of the system can be expressed as

$$Y_p = S_x\Delta x_i(k) + I_y(k) + S_w\Delta w_i(k) + S_u\Delta U_i(k) \quad (12)$$

where Y_p represents the p -step prediction output vector of the system and can be expressed as

$$Y_p = [y(k+1|k) \ y(k+2|k) \ \dots \ y(k+p|k)]^T \quad (13)$$

and S_x , I , S_w , and S_u represent the recursive coefficient matrix of the state increment, output increment, measured disturbed increment, and input increment, respectively.

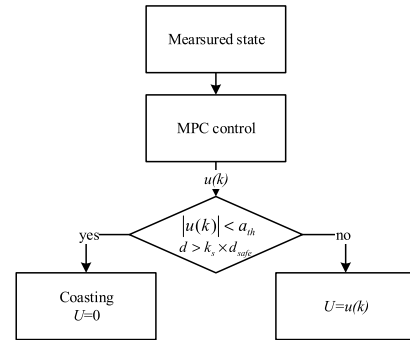


FIGURE 4. Coasting strategy process diagram.

TABLE 1. Train parameters.

Train type	Formation	Length (m)	Maximum acceleration (m/s^2)	Maximum brake acceleration (m/s^2)
CBTC	4 B	2M2T	1.08	1
VCTF	3 B	2M1T	1.08	1

TABLE 2. Simulation parameter value.

MPC Parameter	Default Value
m	10
p	3
T_s	100 ms
d_0	6 m
k_t	3
τ	1
Q	diag{0.8,0.4,0.6}

B. MPC OPTIMIZATION PROBLEM

The evaluation functions must achieve the following objectives: 1) the steady-state tracking error is zero; 2) the changing acceleration rate of the train is as low as possible to ensure riding comfort; and 3) the output command should avoid frequent switching between traction and braking, thereby reducing energy consumption.

The tracking error index of train i at step k can be calculated using the distance error $\Delta d_i(k)$ and the velocity error $\Delta v_i(k)$. The riding comfort can be calculated by the rate of change in the train acceleration:

$$j_i(k) = (a_i(k) - a_i(k-1)) / T_s \quad (14)$$

The optimization objective function is constructed using the weighted summation of the three indices of the spacing error, velocity error, and jerk and can be expressed as follows:

$$\min J = \sum_{i=1}^p \|Q_{y,i}y_{i,c}(k+i|k)\|^2 \quad (15)$$

where $Q_{y,i} = \text{diag}\{q_d, q_v, q_j\}$ is the weighted coefficient matrix of the controlled output index $y_{i,c}$.

The following constraints should be considered to ensure the operational safety and performance of each train in the platoon.

- 1) Safety Stopping Constraint: The distance between two adjacent trains in the platoon should be larger than the relative

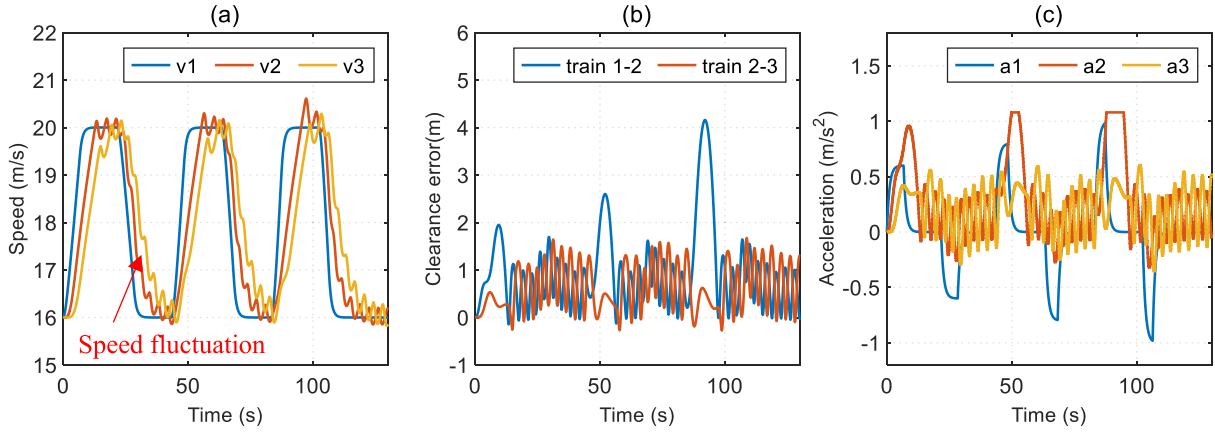


FIGURE 5. Simulation results of the PD controller. (a) Vehicle velocity. (b) Clearance error. (c) Acceleration.

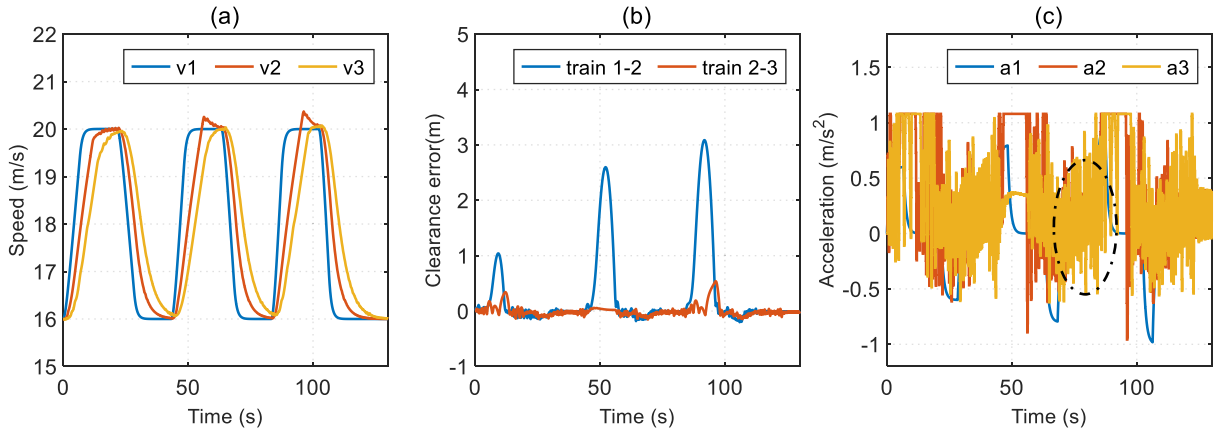


FIGURE 6. Simulation results of the MPC controller. (a) Vehicle velocity. (b) Clearance error. (c) Acceleration.

braking distance, ensuring that each train in the platoon can stop safely in an emergency scenario. The following equation should be satisfied:

$$\frac{v_{i-1}^2(k)}{2a_{b\max(i-1)}} - \frac{v_i^2(k)}{2a_{b\max(i)}} + d_i(k) > 0 \quad (16)$$

where $a_{b\max(i)}$ and $a_{b\max(i-1)}$ are the maximum braking accelerations of trains i and $i-1$, respectively.

2) Line Velocity Constraint: The train operation speed should be lower than the line limit speed to avoid train derailment, and the speed of train i can be limited as

$$v_i(k) < v_{\text{line}}(k) \quad (17)$$

We assume that the line limit speeds of trains i and $i-1$ are unchanged in the prediction time domain. Because the speeds of trains i and $i-1$ satisfy the constraints of Eq. (17), we can obtain that $v_i(k) + v_{i-1}(k) < 2 \times v_{\text{line}}(k)$. In addition, the prediction domain is finite; it can be derived that $v_i(k) + v_{i-1}(k) < 2 \times (v_i(k) + a_{\max} \times T_s \times p)$, where $v_i(k)$ is the maximum of $v_i(k)$ and $v_{i-1}(k)$, and a_{\max} is the maximum acceleration of trains i and $i-1$. The constraint of Eq. (16) can then be simplified to a linear constraint and expressed as

$$d_i(k) > \frac{v_{\text{limit}}}{a_{b\max}} \Delta v_i(k) \quad (18)$$

where $a_{b\max} = \min \{a_{b\max(i)}, a_{b\max(i-1)}\}$, and $v_{\text{limit}} = \min\{v_{\text{line}}(k), v_i(k) + a_{\max} \times T_s \times p\}$. The constrained output can be expressed as $y_{i,d}(k) = [\Delta d_i(k) \Delta v_i(k) v_i(k)]^T$.

3) Train Performance Constraint: In addition to considering the constraints of safe operation, it is necessary to consider the instruction limitation of the traction and braking transmission system. Therefore, input constraints are included and can be described as follows. Because the maximum train acceleration and deceleration are limited in practice, the control command range of the traction and braking transmission system is restricted as

$$\begin{cases} a_{i\min} \leq u_i(k) \leq a_{i\max} \\ j_{i\min} \leq \Delta u_i(k) \leq j_{i\max} \end{cases} \quad (19)$$

where $a_{i\min}$, $a_{i\max}$, $j_{i\min}$, and $j_{i\max}$ are the minimum and maximum accelerations and changing rates of the train acceleration, respectively.

4) String Stability Constraint: The peak magnitude of the deviation from equilibrium spacing should not be amplified through the vehicle string to ensure the stability of the platoon. According to [20], the platoon l_∞ string stable constraint can be expressed as

$$\Delta d_{i-1}^- \leq \Delta d_i(k+h) \leq \Delta d_{i-1,k+1}^+ \quad \forall h \in P \quad (20-a)$$

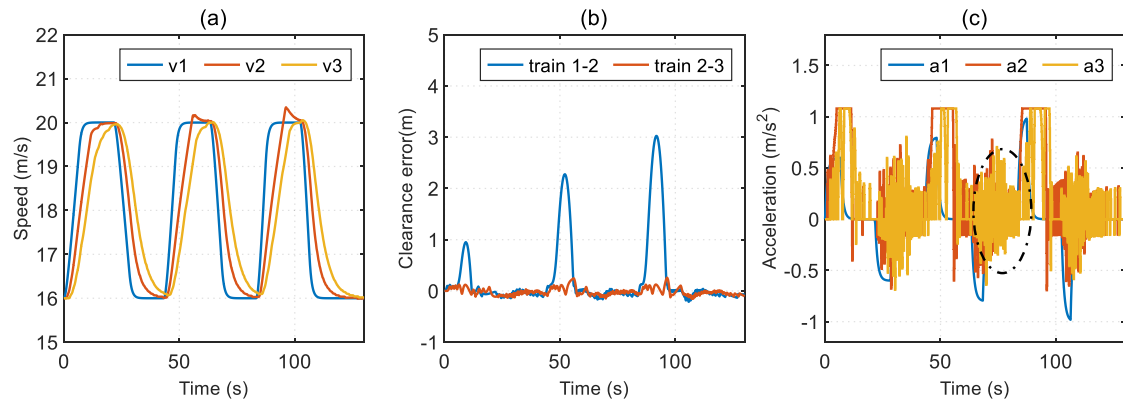


FIGURE 7. Simulation results of the MPC controller with the coasting strategy. (a) Vehicle velocity. (b) Clearance error. (c) Acceleration.

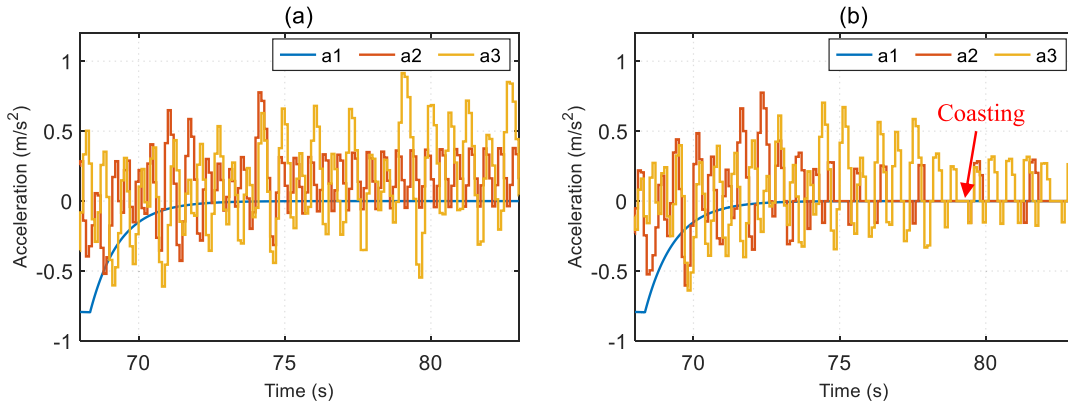


FIGURE 8. Enlarged images of the elliptical dash line area in Figs. 6(c) and 7(c). (a) MPC without the coasting strategy. (b) MPC with the coasting strategy.

$$\Delta d_{i=1,k+1}^- = \begin{cases} -d_0 & \text{for } i = 1 \\ -\max(|\Delta d_{i-1,\mu}^r|) & \text{for } i > 1 \quad \forall \mu \in K \end{cases} \quad (20-\text{b})$$

$$\Delta d_{i-1,k+1}^+ = \max(|\Delta d_{i-1,\mu}^r|) \text{ for } i > 1 \quad \forall \mu \in K \quad (20-\text{c})$$

where $P = \{1, 2, 3, \dots, p\}$, $K = \{0, 1, 2, \dots, k + 1\}$, and $\Delta d_{i-1,\mu}^r$ denotes the actual distance error of train $i - 1$ at time μ . As constraint 1) ~ 3) are more significant concerns compared to constraint 4), the string stability constraint should be softened if there is no feasible solution.

The virtually coupled formation train control strategy is transformed into a quadratic programming problem with constraints and described by Eqs. (14), (17-20).

C. COASTING STRATEGY

A coasting strategy is proposed further to optimize the driving performance of disturbed train modules. By adding a coasting mode, the number of switches between the traction and braking states and the operational energy consumption can be reduced. This switch coasting strategy is shown in Fig. 4. When the output command of the MPC is smaller than the threshold and the distance of the train is safe, the train coasts to reduce energy consumption.

In Fig. 4, k_s is the safety distance coefficient, and a_{th} is the acceleration threshold of the coasting.

In each control cycle, the absolute value of the controller output $u(k)$ is calculated, and the safe distance d_{safe} is calculated by Eq. (18). If the switch conditions in Fig. 4 are satisfied, the coasting strategy is applied. Conversely, if the output control command of the MPC is beyond the threshold value or the train spacing does not meet the safety margin, the train control command applies the MPC output.

IV. CASE STUDY

Numerical experiments using MATLAB/SIMULINK are conducted to analyze the proposed method. First, the tracking performance of three train modules based on the proposed method is investigated. Next, VCTF is applied to the Beijing Metro Yanfang Line to test the operational capability of the virtually coupled train formation.

A. SIMULATION PARAMETERS

There are nine stations on the Yanfang Line, and the length of the line is 14.4 km. The maximum line limit speed is 80 km/h. The train parameters are listed in Table 1. Currently, the signal system is CBTC, and the train formation is 2M2T, wherein M represents the motor vehicle, and T represents the trailer vehicle. Considering the motor vehicle utilization, the single-train module in the VCTF is 2M1T.

The train modules are simulated using Eqs. (1) and (2). According to [23], the basic running resistance coefficient of type B train is as follows: $a = 1.08$, $b = 0.008$, and

TABLE 3. Performance index comparison of different control strategies.

Control method	Train id	Distance error	Speed error	Jerk	Energy cost
PD	2	125.1	79.76	3.757	2222
	3	83.27	76.11	4.168	2047
MPC	2	43.32	76.74	4	1025
	3	8.394	71.1	4.506	908.2
MPC with coasting	2	41.29	76.25	2.519	723.9
	3	7.932	70.91	2.804	574.3

$c = 0.0096$. The time delay constant of the traction and braking system is 1.0 second. The time distance coefficient should satisfy the condition $k_t > 2 \times \tau$ to ensure string stability according to [24], so the constant time distance k_t is 3. The control strategy for the virtually coupled formation train is transformed into the optimization problem presented in Section III. The MPC parameter value is shown in Table 2.

Additionally, to analyze the control performance of the MPC controller designed in this study, an automobile adaptive cruise car PD controller provided in [25] is simulated for comparison:

$$u_i = k_1 \times (s_i - s_{i-1} - k_t \times v_i - d_0) + k_2 \times (v_i - v_{i-1}) \quad (21)$$

where $k_1 = 0.33$, and $k_2 = 0.25$.

B. PERFORMANCE OF THE VCTF CONSIDERING SPEED CHANGES IN THE LEADER TRAIN

In this part, three train modules form a virtually coupled train formation. The leader train speed changes according to the set speed curve. The tracking process of the follower train 2 and train 3 under the MPC and PD controller are simulated and analyzed. The initial speed of each train is 16 m/s, and the initial spacing error is zero. First, the leader train 1 speeds up to 20 m/s at 0.6 m/s^2 , operates at a constant speed for 15 s, decreases its speed to 16 m/s at -0.6 m/s^2 , and maintains a uniform speed for 15 s. In the second velocity cycle, train 1 repeats acceleration–uniform–deceleration–uniform process, and the acceleration magnitude and deceleration magnitude increase from 0.6 m/s^2 to 0.8 m/s^2 . The initial and maximum velocities are the same as those in the first circle. The acceleration magnitude and deceleration magnitude of the third cycle is 1.0 m/s^2 . The simulation tracking process of train 2 and train 3 under the PD, MPC, and MPC with the coasting strategy are shown in Figs. 5–7, respectively. The simulation platform is an industrial computer with 3.7-GHz CPU and 128-GB memory. The peak and mean computing time to solve MPC are 59.9 ms and 0.3578 ms, which are lower than the fixed time step ($T_s = 100 \text{ ms}$).

Figs. 5 and 6 show that train 2 and train 3 can follow the speed change of train 1 with some delay, and the space error of each train is within 5 meters. In each velocity cycle, the maximum clearance error of train 3 is less than train 2, thus indicates the maximum distance error decreases according to the platoon and shows the l_∞ string stability. Compared with the PD controller, the speed curve of the MPC is smoother with

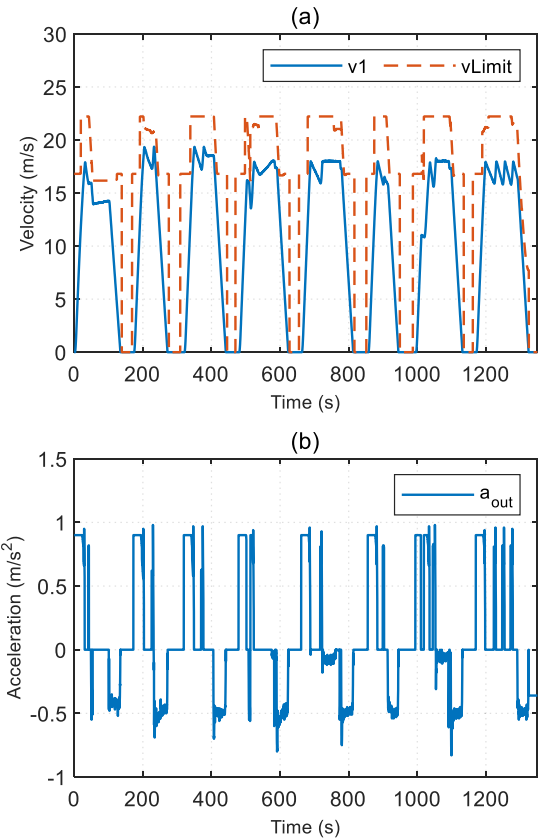


FIGURE 9. Actual operation velocity and ATO output command curve of the Yanfang Line. (a) Vehicle velocity. (b) Acceleration output.

minor delay according to the speed of train 1. The distance error of the MPC is lower than that of the PD controller. The simulation results indicate that the MPC performs better than the PD controller in tracking the leader train. The MPC considers the motion of the leader train during the predictive time, so the speed fluctuation regulation is decreased compared with the PD controller, which ensures excellent tracking performance. Moreover, the MPC is feasible during the simulation time, ensuring the constraints of Eqs. (17–20) are satisfied.

In Figs. 5(c) and 6(c), a_1 indicates the operation acceleration for train 1, whereas a_2 and a_3 is the desired acceleration calculated by the MPC or PD controller. Because of the train running resistance in Eq. (2), a_2 is not zero when train 2 operates at a constant speed. A comparison of Figs. 5(c) and 6(c) show that the MPC controller regulation frequency between acceleration and deceleration is more extensive than that of the PD controller, especially in the area marked by the elliptical dash line. In train actual operation, the response time from braking to traction is longer according to the safety constraint. Moreover, the regulation between traction and braking increases the running energy costs. To ensure running performance and safety, the controller should minimize the switching times between acceleration and deceleration. The coasting strategy presented in Section III.C is applied to reduce the MPC frequency regulation, and the result is shown in Figs. 7. The velocity error and clearance error change

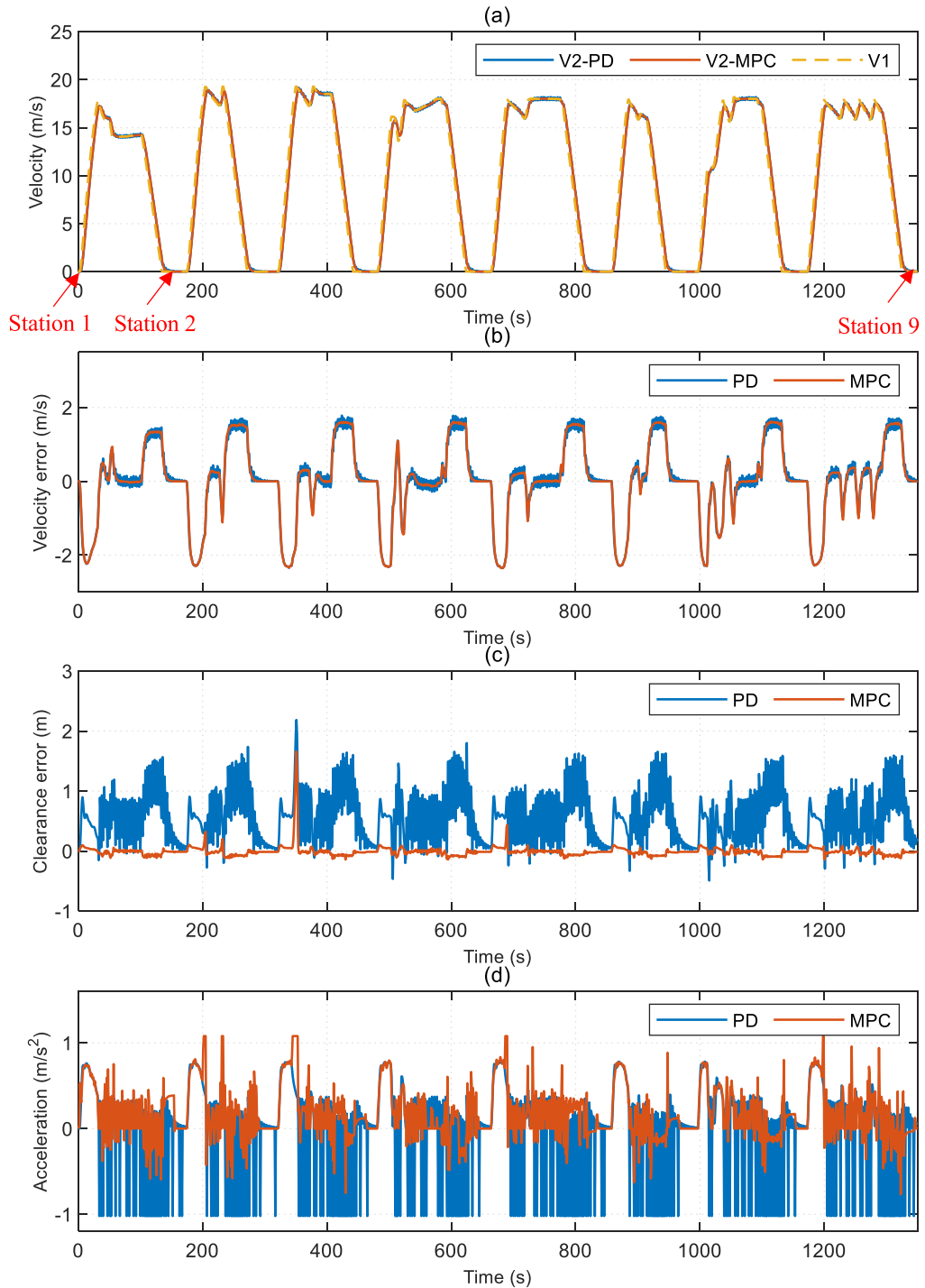


FIGURE 10. Actual operation velocity and ATO output command curve of the Yanfang Line. (a) Vehicle velocity. (b) Velocity error. (c) Clearance error. (d) Acceleration output.

little under the coasting strategy. Simultaneously, the switch times between acceleration and deceleration are significantly decreased, as shown in Fig. 8. A comparison of Figs. 6 and 7 indicates that the coasting strategy can reduce the regulation frequency between traction and braking and enhance the train running performance.

The space error index, speed error index, jerk index, and energy consumption index are calculated to analyze the performance of the three control methods quantitatively.

The calculation method for each index is as follows:

$$\left\{ \begin{array}{l} \text{clearance error} = \int_0^{t_{end}} |d(t) - d_{des}(t)| dt \\ \text{speed error} = \int_0^{t_{end}} |v_i(t) - v_{i-1}(t)| dt \\ \text{jerk} = \int_0^{t_{end}} |j_i(t)| dt \\ e_cost = \int_0^{t_{end}} \frac{\text{sgn}(u_i(t)) + 1}{2} \times u_i(t) \times v_i(t) dt \end{array} \right. \quad (22)$$

TABLE 4. The capacity comparison.

	Rush hour			Low-traffic period		
	Carriages number	Departure time (min)	Train capacity (p/h) ^a	Carriages number	Departure time (min)	Train capacity (p/h)
CBTC	4	5	11520	4	8	7200
VCTF	6	5	17040	3	6	7100

^a p/h = passengers per hour

where t_{end} is the simulation time, e_cost is the energy cost index, and $sgn()$ is the sign function. Because the metro train applies resistance braking, there is no energy consumption or recycling with the power grid when the train brakes. Therefore, the energy consumption index is calculated only when the train is experiencing traction. Because the train quality is constant for each controller, its value is set as 1 to simplify the calculation. The calculation results are presented in Table 3.

Table 3 shows the performance index value of the following train 2 and train 3 for each control experiment. The results show that the distance error of the PD controller is almost three times that of the MPC, and the speed error value is nearly the same. The jerk of the MPC is worse than the PD controller. The index values of MPC with coasting express that the coasting strategy can guarantee track performance with lower energy consumption and jerk, which improves the driving performance of MPC.

C. SIMULATION OF VCTF OPERATION ON THE YANFANG LINE

A simulation experiment on the Beijing Metro Yanfang Line is presented to validate the performance of the proposed method. The actual operating speed and line limit speed are shown in Fig. 9(a), and the acceleration command by ATO is illustrated in Fig. 9(b). Within the length constraints of the existing platform, VCTF adopts two train modules to form a platoon during rush hour and a single-train module operation in a flat hour.

We assume that leader train 1 operates per the ATO speed curve, as shown in Fig. 9(a), and train 2 operates under the MPC controller with the coasting control strategy proposed in Section III. The running process of train 2 is simulated, and the experimental results between stations are shown in Fig. 10.

The speed curve of train 2 synchronously follows leader train 1 from station 1 to station 9, as shown in Fig. 10(a). Fig. 10(b) and 10(c) indicate the increases in speed error and clearance error when train 1 accelerates or decelerates, especially near the train station. Because the acceleration of train 1 is assumed to be constant during the MPC predicted domain, the tracking performance deteriorates when the acceleration of train 1 changes rapidly. Owing to the traction/braking system delay, the tracking error of the PD controller is even worse. The delayed arrival time between train 2 and train 1 cannot be canceled as a safety constraint. Fig. 10(c) and 10(d) show that the output acceleration of the MPC is smaller than that of the PD controller, while the clearance error of the MPC is smaller than that of the PD controller. It can be concluded

that the proposed MPC control method can achieve superior running performance with lower acceleration compared to the PD controller.

The capacity of VCTF and CBTC is analyzed to evaluate the operational improvement obtained by the VCTF. The comparison results are presented in Table 4. Because the number of carriages in a VCTF is 1.5 times that of a CBTC signal system train, the passenger capacity during rush hour can be improved by a factor of 1.47 by VCTF under the current line and station platform conditions. Additionally, during low-traffic hours, there is one train module in a VCTF such that the passenger occupancy rate can be improved, and the train departure time decrease to 6 min, which can enhance the quality of passenger service.

V. SUMMARY AND DISCUSSION

This paper proposes a VCTF train control method based on an MPC framework to achieve cooperative control of virtually coupled metro trains. First, a dynamic model of virtually coupled trains is introduced, and the output state is predicted using this model. We choose the train track spacing error, velocity error, and riding comfort as the control objectives, and the objective function is obtained based on a weighted method. The platoon collision avoidance constraint is derived and transformed into a linear constraint. Additionally, the line speed constraint, traction/braking system limitation, and string stability constraint are considered. Finally, the virtually coupled train control problem is converted into a constrained quadratic programming problem and solved by the active-effective-set method. Besides, a coasting strategy is proposed to improve the output of the MPC and reduce driving energy consumption.

Experimental results validate the performance improvement of the proposed MPC method and coasting strategy. The simulation results show that the proposed MPC approach achieves excellent tracking ability compared with the PD controller. During simulation time, the feasibility of MPC shows the safety running constraint is satisfied, which is essential for the platoon. The coasting strategy increases slide time and reduces driving energy consumption significantly. The Yanfang Line simulation results indicate that the following train controlled by the proposed approach operates on the line with a tiny tracking error, and VCTF can improve the metro peak capacity in rush hour and service quality during low-traffic periods.

Future research about the cooperation control effects for different train types is desired. Other important issues include communication delay and topology, which are ongoing research subjects.

REFERENCES

- [1] F. Flaminini, S. Marrone, R. Nardone, A. Petrillo, S. Santini, and V. Vittorini, "Towards railway virtual coupling," in *Proc. IEEE Int. Conf. Electr. Syst. Aircr. Railway Ship Propuls. Road Vehicles Int. Transp. Electricr. Conf. (ESARS-ITEC)*, Nottingham, U.K., Nov. 2018, pp. 1–6, doi: [10.1109/ESARS-ITEC.2018.8607523](https://doi.org/10.1109/ESARS-ITEC.2018.8607523).
- [2] I. Mitchell, "ERTMS level 4, train convoys or virtual coupling," IRSE, London, U.K., Tech. Rep., 2016, no. 219, pp. 14–15. [Online]. Available: <https://webinfo.uk/webdocssl/irse-kbase/ref-viewer.aspx?Refno=1882928268&document=ITC%20Report%2039%20Train%20convoys%20and%20virtual%20coupling.pdf>
- [3] C. Wang, S. Gong, A. Zhou, T. Li, and S. Peeta, "Cooperative adaptive cruise control for connected autonomous vehicles by factoring communication-related constraints," *Transp. Res. C, Emerg. Technol.*, vol. 113, pp. 124–145, Apr. 2020, doi: [10.1016/j.trc.2019.04.010](https://doi.org/10.1016/j.trc.2019.04.010).
- [4] Y. Zhou and S. Ahn, "Robust local and string stability for a decentralized car following control strategy for connected automated vehicles," *Transp. Res. B, Methodol.*, vol. 125, pp. 175–196, Jul. 2019, doi: [10.1016/j.trb.2019.05.003](https://doi.org/10.1016/j.trb.2019.05.003).
- [5] S. Konig and U. Herbst, "Virtually coupled train formations—an approach for enhancing freight rail traffic," presented at the 8th World Congr. Intell. Transp. Syst., Sydney, NSW, Australia, Sep. 2001.
- [6] U. Bock and G. Bikker, "Design and development of a future freight train concept—'Virtually coupled train formations,'" *IFAC Proc. Volumes*, vol. 33, no. 9, pp. 395–400, Jun. 2000, doi: [10.1016/S1474-6670\(17\)38176-4](https://doi.org/10.1016/S1474-6670(17)38176-4).
- [7] J. Aoun, E. Quaglietta, and R. Goverde, "Investigating market potentials and operational scenarios of virtual coupling railway signaling," *Transp. Res. Rec.*, vol. 2674, no. 8, pp. 799–812, 2020, doi: [10.1177/0361198120925074](https://doi.org/10.1177/0361198120925074).
- [8] Y. Zhang and H. Wang, "Topological manifold-based monitoring method for train-centric virtual coupling control systems," *IET Intell. Transp. Syst.*, vol. 14, no. 2, pp. 91–102, Feb. 2020, doi: [10.1049/iet-its.2019.0330](https://doi.org/10.1049/iet-its.2019.0330).
- [9] G. Munandi, "Blockchain-enabled virtual coupling of automatic train operation fitted mainline trains for railway traffic conflict control," *IET Intell. Transp. Syst.*, vol. 14, no. 6, pp. 611–619, Jun. 2020, doi: [10.1049/iet-its.2019.0694](https://doi.org/10.1049/iet-its.2019.0694).
- [10] C. D. Meo, M. D. Vaio, F. Flaminini, R. Nardone, S. Santini, and V. Vittorini, "ERTMS/ETCS virtual coupling: Proof of concept and numerical analysis," *IEEE Trans. Intell. Transp. Syst.*, vol. 21, no. 6, pp. 2545–2556, Jun. 2020, doi: [10.1109/TITS.2019.2920290](https://doi.org/10.1109/TITS.2019.2920290).
- [11] E. Quaglietta, M. Wang, and R. M. P. Goverde, "A multi-state train-following model for the analysis of virtual coupling railway operations," *J. Rail Transp. Planning Manage.*, vol. 15, Sep. 2020, Art. no. 100195, doi: [10.1016/j.jrtpm.2020.100195](https://doi.org/10.1016/j.jrtpm.2020.100195).
- [12] J. Felez, Y. Kim, and F. Borrelli, "A model predictive control approach for virtual coupling in railways," *IEEE Trans. Intell. Transp. Syst.*, vol. 20, no. 7, pp. 2728–2739, Jul. 2019, doi: [10.1109/TITS.2019.2914910](https://doi.org/10.1109/TITS.2019.2914910).
- [13] S. Li, L. Yang, and Z. Gao, "Distributed optimal control for multiple high-speed train movement: An alternating direction method of multipliers," *Automatica*, vol. 112, Feb. 2020, Art. no. 108646, doi: [10.1016/j.automatica.2019.108646](https://doi.org/10.1016/j.automatica.2019.108646).
- [14] R. Parise, H. Dittus, J. Winter, and A. Lehner, "Reasoning functional requirements for virtually coupled train sets: Communication," *IEEE Commun. Mag.*, vol. 57, no. 9, pp. 12–17, Sep. 2019, doi: [10.1109/MCOM.2019.1800936](https://doi.org/10.1109/MCOM.2019.1800936).
- [15] V. Turri, B. Besselink, and K. H. Johansson, "Cooperative look-ahead control for fuel-efficient and safe heavy-duty vehicle platooning," *IEEE Trans. Control Syst. Technol.*, vol. 25, no. 1, pp. 12–28, Jan. 2017, doi: [10.1109/TCST.2016.2542044](https://doi.org/10.1109/TCST.2016.2542044).
- [16] A. Duret, M. Wang, and A. Ladino, "A hierarchical approach for splitting truck platoons near network discontinuities," *Transp. Res. B, Methodol.*, vol. 132, pp. 285–302, Feb. 2020, doi: [10.1016/j.trb.2019.04.006](https://doi.org/10.1016/j.trb.2019.04.006).
- [17] C. Zhai, Y. Liu, and F. Luo, "A switched control strategy of heterogeneous vehicle platoon for multiple objectives with state constraints," *IEEE Trans. Intell. Transp. Syst.*, vol. 20, no. 5, pp. 1883–1896, May 2019, doi: [10.1109/TITS.2018.2841980](https://doi.org/10.1109/TITS.2018.2841980).
- [18] C. Zhai, X. Chen, C. Yan, Y. Liu, and H. Li, "Ecological cooperative adaptive cruise control for a heterogeneous platoon of heavy-duty vehicles with time delays," *IEEE Access*, vol. 8, pp. 146208–146219, 2020, doi: [10.1109/ACCESS.2020.3015052](https://doi.org/10.1109/ACCESS.2020.3015052).
- [19] M. Wang, "Infrastructure assisted adaptive driving to stabilise heterogeneous vehicle strings," *Transp. Res. C, Emerg. Technol.*, vol. 91, pp. 276–295, Jun. 2018, doi: [10.1016/j.trc.2018.04.010](https://doi.org/10.1016/j.trc.2018.04.010).
- [20] Y. Zhou, M. Wang, and S. Ahn, "Distributed model predictive control approach for cooperative car-following with guaranteed local and string stability," *Transp. Res. B, Methodol.*, vol. 128, pp. 69–86, Oct. 2019, doi: [10.1016/j.trb.2019.07.001](https://doi.org/10.1016/j.trb.2019.07.001).
- [21] L. Xiao, M. Wang, and B. van Arem, "Realistic car-following models for microscopic simulation of adaptive and cooperative adaptive cruise control vehicles," *Transp. Res. Rec., J. Transp. Res. Board*, vol. 2623, no. 1, pp. 1–9, Jan. 2017, doi: [10.13141/2623-01](https://doi.org/10.13141/2623-01).
- [22] X. Jin, J. Yang, Y. Li, B. Zhu, J. Wang, and G. Yin, "Online estimation of inertial parameter for lightweight electric vehicle using dual unscented Kalman filter approach," *IET Intell. Transp. Syst.*, vol. 14, no. 5, pp. 412–422, May 2020, doi: [10.1049/iet-its.2019.0458](https://doi.org/10.1049/iet-its.2019.0458).
- [23] W. Chen, Q. Zhu, and L. Li, "CBTC based urban rail transit train energy consumption algorithm and simulation," *Appl. Res. Comput.*, vol. 28, no. 6, p. 2127, 2011, doi: [10.3969/j.issn.1001-3695.2011.06.034](https://doi.org/10.3969/j.issn.1001-3695.2011.06.034).
- [24] R. Rajamani, "Longitudinal control for vehicle platoons," in *Vehicle Dynamics and Control*, 2th ed. Boston, MA, USA: Springer, 2012, pp. 171–200.
- [25] V. Milanés and S. E. Shladover, "Modeling cooperative and autonomous adaptive cruise control dynamic responses using experimental data," *Transp. Res. C, Emerg. Technol.*, vol. 48, pp. 285–300, Nov. 2014, doi: [10.1016/j.trc.2014.09.001](https://doi.org/10.1016/j.trc.2014.09.001).



ZIYU WU received the Ph.D. degree in electrical engineering from the Chinese Academy of Sciences, Beijing, China, in 2016.

She currently holds a postdoctoral position with the School of Electronics and Information Engineering, Beijing Jiaotong University, and also with Traffic Control Technology Company Ltd., Beijing. Her current research interests include virtually coupled train control method, train traction/braking system modeling approach, and intelligent control systems.



CHUNHAI GAO received the B.S. degree in railway signals from Northern Jiaotong University, Beijing, China, in 1993, and the M.S. degree in traffic information and control from Beijing Jiaotong University, in 2003.

He is currently a Professor and the Director of the National Engineering Research Center of Rail Transit Operation Control System, Beijing Jiaotong University. His research interests include communication-based train control and high-speed train control systems.



TAO TANG (Senior Member, IEEE) received the Ph.D. degree in automatic control theory and application from the Chinese Academy of Sciences, Beijing, China, in 1991.

He is currently a Professor with the School of Electronics and Information Engineering and the Director of the State Key Laboratory of Rail Traffic Control and Safety, Beijing Jiaotong University, Beijing. His current research interests include communication-based train control, high-speed train control, and intelligent control theory and systems.

Dr. Tang is also a Specialist with the National Development and Reform Commission and the Beijing Urban Traffic Construction Committee.